Application of a Logarithmic Complementary Metal–Oxide–Semiconductor Camera in White-Light Interferometry

Patrick Egan, Fereydoun Lakestani, Maurice P. Whelan, and Michael J. Connelly, *Member, IEEE*

***Abstract*—This paper describes the characterization, modeling, and application of a direct-readout complementary metal–oxide–semiconductor (CMOS) camera in white-light interferometry (WLI). The camera that was used consisted of a direct-readout 1024 × 1024 pixel logarithmic CMOS sensor. A continuous analog voltage from each pixel was converted to an 8-bit value by an internal analog-to-digital converter and processed with a digital signal processor. A mathematical model relating the input light intensity to the 8-bit digitized output is developed, which is critical in applications where knowledge of the scene intensity is essential to estimating the maximum allowable frame rates. The camera was utilized in WLI, and its application is analyzed in terms of maximum output signal amplitude, imaging speed, and light intensity. The mathematical modeling is implemented with SPICE simulations and verified with experimental data.**

***Index Terms*—Calibration, cameras, complementary metal–oxide–semiconductor field effect transistors (CMOSFETs), machine vision, modeling, optical interferometry.**

I. Introduction

OFFERING extremely fast frame rates, large dynamic range, random pixel access, and onboard digitization and processing, the direct-readout logarithmic complementary metal–oxide–semiconductor (CMOS) and digital signal processor (DSP) camera is an inexpensive and versatile imaging device that is ideally suited for full-field machine vision and optical metrology applications. However, a pixel time response that is dependent on light intensity, substantial noise levels, and a logarithmic response imposes significant restrictions on its use in white-light interferometry (WLI).

Manuscript received August 26, 2005; revised March 9, 2007. This work was supported in part by the University of Limerick Foundation and by the Enterprise Ireland International Collaboration Grant. This work was undertaken within the framework of a Collaboration Agreement (No. 18697-2001-1 SOSC ISP IE) between the University of Limerick, Ireland, and the Institute for Health and Consumer Protection, European Commission Directorate General Joint Research Centre, Italy.

P. Egan and M. J. Connelly are with the Optical Communications Research Group, Department of Electronic and Computer Engineering, University of Limerick, Limerick, Ireland (e-mail: michael.connelly@ul.ie).

F. Lakestani is with the Photonics Sector, Institute for Health and Consumer Protection, European Commission Joint Research Centre, 21020 Ispra, Italy.

M. P. Whelan is with the Photonics Sector, Institute for Health and Consumer Protection, European Commission Joint Research Centre, 21020 Ispra, Italy, and also with the Stokes Research Institute, University of Limerick, Limerick, Ireland (e-mail: maurice.whelan@jrc.it)

Color versions of one or more of the figures in this paper are available online at http://ieeexplore.ieee.org.

Digital Object Identifier 10.1109/TIM.2007.907962

In a previous work [1], the application of a logarithmic CMOS-DSP camera (iMVS-155, AKAtech SA, CH) to full-field WLI was demonstrated. The electronic pixel scanning of the CMOS sensor proved to be an effective and inexpensive alternative to the complex electromechanical scanning of the sample under test. Using a Michelson interferometer and an 830-nm superluminescent diode light source supplying 3.6 mW of power, a 3-D reconstruction of a rough aluminum surface was achieved with lateral and axial resolutions of 14 and 14 μm, respectively. The intention of the work was to utilize the camera as an imaging device for full-field optical coherence tomography [2]; however, with an unprocessed signal-to-noise ratio of approximately 3 from the surface of the aluminum sample, the subsurface imaging of a highly scattering sample proved to be unfeasible. The purpose of this paper is to provide a comprehensive model of the camera and through this model identify the limitations of the logarithmic CMOS-DSP camera in WLI.

Most CMOS image sensors can be classified as either linear or logarithmic. The pixel of the linear CMOS image sensor typically incorporates a reset signal, and by charging and resetting, it achieves an integration of input light photons to produce a linear output voltage response to light intensity. The logarithmic CMOS image sensor features a logarithmic resistive load that continuously produces a logarithmic output voltage to input photocurrent. This nonintegrating response of the logarithmic CMOS image sensor allows the continuous measurement of the logarithmic output voltage in time (hence the term "direct readout"). Combined with true random pixel access in space, the direct-readout sensor can access a small pixel region of interest with reduced processing time and permits very fast frame rates (e.g., 64 × 1 pixels at 1900 Hz).

The logarithmic CMOS image sensor [3] and the CMOS-DSP camera [4] are very suitable for industrial machine vision use since they provide good image quality with a large dynamic range and fast frame rates. These features proved to be invaluable in a real-time welding application where linear charge-coupled-device (CCD) cameras saturated [5]. When a logarithmic CMOS camera was applied to speckle interferometry [6] and compared to CCD-based systems, it was found that although the CMOS sensor suffered from higher noise levels, its fast frame rates and large dynamic range were attractive to the optical metrology of samples with a wide-ranging reflectivity. Furthermore, a logarithmic CMOS-DSP camera was employed in a full-field laser interferometry [7], where it

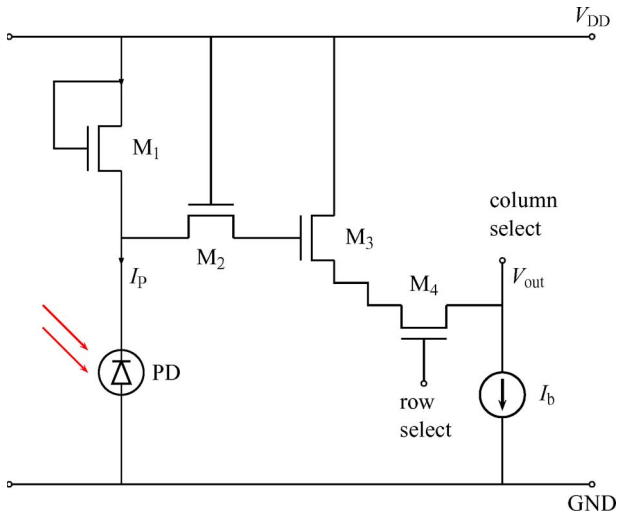

Fig. 1. Direct-readout CMOS pixel. MOSFET M_1 acts as a logarithmic resistive load that gives a logarithmic response to light intensity.

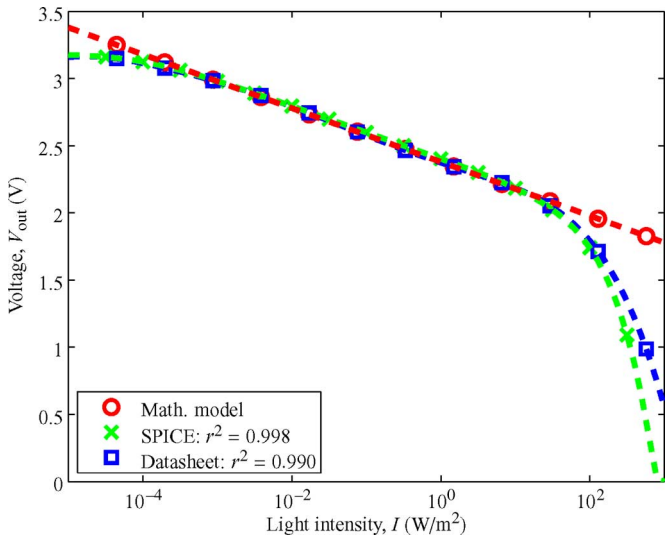

Fig. 2. Output voltage of the CMOS sensor as a function of input light intensity. The mathematical model has $m = -200.076 \times 10^{-3}$ V/dB and $I_0 = 1.0 \times 10^{11.89}$ W/m^2.

achieved displacement measurements comparable in sensitivity to a commercial laser Doppler vibrometer.

A detailed model of fixed pattern noise in a logarithmic CMOS camera that suggested calibration and correction techniques for fixed pattern noise reduction was reported [8]. This paper models a logarithmic CMOS-DSP camera and its application to WLI. Section II develops a model that uses least-squares minimization to relate the light intensity on the sensor to the output digitized value, which thus allows the quick and accurate estimation of the pixel response time. From this model, Section III analyzes the limitations of the camera in WLI with particular emphasis on optical coherence tomography.

II. Characterization of the Logarithmic CMOS Sensor

A. CMOS Pixel Output Voltage

The relationship between the CMOS pixel output voltage and the input light intensity is logarithmic due to the diode-connected NMOS transistor M_1 that acts as a logarithmic resistive load to the pixel photocurrent, as shown in Fig. 1. The output voltage response to light intensity I can be modeled as

$$V_{\text{out}} = m \log_{10}\left(\frac{I}{I_0}\right) \tag{1}$$

where m and I_0 are constants, namely the voltage sensitivity per decade and the intensity value at which $V_{\text{out}} = 0$, respectively. The squared correlation coefficient r^2 between the model of (1) and the SPICE simulation and data sheet response is presented in Fig. 2 for the light intensity range of 1×10^{-4} to 1×10^{2} W/m^2. The mathematical model becomes inaccurate when at low intensities M_1 cuts off and at high intensities M_1 enters the linear mode of operation.

The SPICE simulations were performed with the software package OrCAD v9.2. The MOSFET level 7 model (BSIM3v3.2.2) was used with a 0.5-μm CMOS process: the MOSFETs width and length were 0.5 μm. The photodiode was modeled using a three-node diode subcircuit, where an output forward current was produced by an input power (light) multiplied by the sensitivity.

B. CMOS Pixel Response Time and Light Intensity

A consequence of the logarithmic resistive load and the capacitance associated with the pixel photodiode and pixel transistors is a pixel response time that is dependent on light intensity. This relationship was experimentally verified by applying a 780-nm laser light to the sensor at various small-signal amplitude-modulated intensities, sweeping the frequency (10 Hz–10 kHz) of the modulation, and calculating the pixel rms digitized output. The pixel response was modeled as a low-pass filter having a frequency response that accounts for incident light intensity defined as

$$H(f) = \frac{1}{\sqrt{1 + \left(\frac{f}{f_c}\right)^2}} = \frac{1}{\sqrt{1 + \left(\frac{f}{\kappa I}\right)^2}} \tag{2}$$

where f_c is the -3-dB cutoff frequency of the response, which is directly related to the input light intensity I by a constant factor κ, which is related to the sensitivity of the CMOS pixel [9]. As shown in Fig. 3, the SPICE simulation correlates with the experimental data and the pixel frequency response model of (2). The cutoff frequency of the pixel increases with increasing light intensity due the decreasing resistance of the logarithmic load. It is important to note that although the CMOS sensor is capable of direct readout and random access at extremely high rates, it is the minimum intensity of interest in the image that determines how fast the pixel will respond.

C. CMOS Output Voltage and Digitized Camera Output

The investigated camera has an 8-bit analog-to-digital converter (ADC) that digitizes the analog output voltage of the CMOS sensor to an integer between 0 and 255. A block diagram of the camera operation and the digitization process

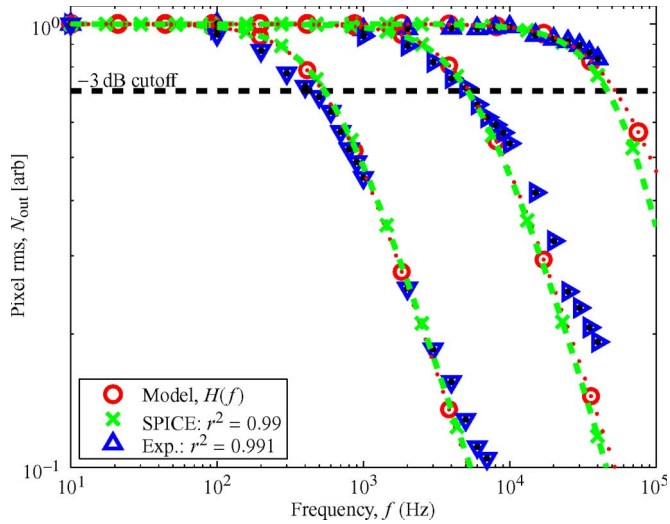

Fig. 3. Frequency response of the CMOS pixel showing that the cutoff frequency increases as the light intensity increases.

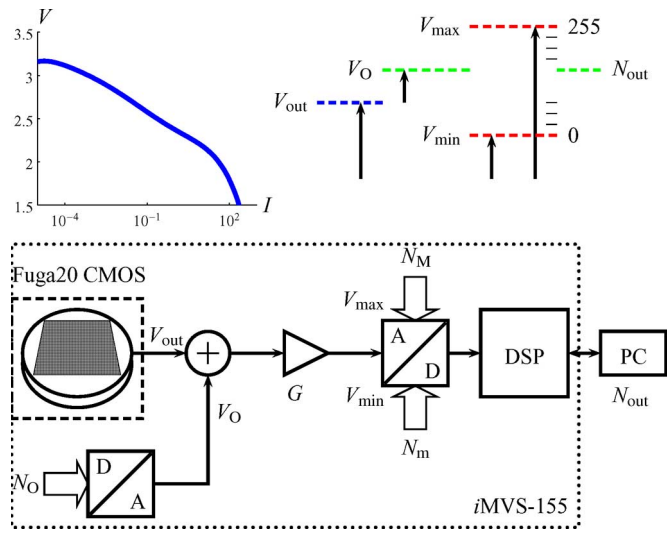

Fig. 4. Digitization process and camera functional block diagram. The analog voltage output from a CMOS pixel is V_{out}. The 8-bit digitized pixel value at the output of the camera is N_{out}.

is shown in Fig. 4. Before arriving at the 8-bit integer N_{out}, an offset voltage V_O is added to the analog voltage of the CMOS sensor V_{out}, as described in (1). This is proceeded by a gain factor G and followed by digitization with 0–255 grayscale levels that correspond to $V_{\min}$ and $V_{\max}$, respectively. Note that the gain has the effect of increasing the voltage range of the digitizer, which therefore decreases the gain acts as an amplification of the pixel output. The relationship between the CMOS sensor analog output voltage and the 8-bit integer at the output of the camera is

$$N_{\text{out}} = 255 - 255\frac{V_{\text{out}} + (C_O - N_O U_O) - (2^G N_m U_m + C_m)}{(2^G N_M U_M + C_M) - (2^G N_m U_m + C_m)} \tag{3}$$

where the subtraction from 255 achieves increasing digitized pixel output with increasing light intensity and will be ignored in the following calculations. The value of N_{out} is dependent on a random pixel-to-pixel offset due to fixed pattern noise. This was corrected for by the subtraction of a calibration uniform gray image and will hence be ignored. However, this assumption is based on the calibration image being taken at a light intensity similar to the normal scene light intensity: a calibration image taken at a different light intensity would introduce error (∼4%) into the following model due to the fixed pattern noise being nonlinearly dependent upon the light intensity [8]. The terms $N_{O,M,m}$ are the known integer values that correspond to the camera setting offset, $\text{ADC}_{\max}$, and $\text{ADC}_{\min}$, respectively. The terms $U_{O,M,m}$ are the unknown voltage spacings for a single integer increase of $N_{O,M,m}$, respectively. The terms $C_{O,M,m}$ are the unknown fixed voltage levels of the camera parameter offset, $\text{ADC}_{\max}$, and $\text{ADC}_{\min}$, respectively. Defining the unknown quantities in matrix form

$$\mathbf{X} = \begin{pmatrix} u_M \\ u_m \\ w \\ v \end{pmatrix} \equiv \begin{pmatrix} \frac{U_M}{U_O} \\ \frac{U_m}{U_O} \\ \frac{C_M - C_m}{U_O} \\ \frac{V + C_O - C_m}{U_O} \end{pmatrix} \tag{4}$$

and substituting into (3), the normalized expression for the output pixel value can be written as

$$n = \frac{N_{\text{out}}}{255} = \frac{v - N_O - 2^G N_m u_m}{2^G N_M u_M - 2^G N_m u_m - w}. \tag{5}$$

The unknown quantities of $\mathbf{X}$ are solved through computational linear algebra [10]. For a fixed value of voltage v, a set of three vectors $\mathbf{N}_O$, $\mathbf{N}_m$, and $\mathbf{N}_M$ of length p is defined, from which p arbitrary estimations of n are deduced, i.e., a vector $\mathbf{n}$. If p is chosen such that the number of equations is greater than the number of unknowns, e.g., $p = 30$, the set of equations is said to be overdetermined. If the closeness of the solution is defined in the least-squares sense, the overdetermined linear problem reduces to a solvable problem called the linear least-squares problem. The quantities u_M, u_m, and w are adjusted to minimize the square of the vector

$$\begin{aligned}\mathbf{A} = \mathbf{n}(2^G \mathbf{N}_M u_M - 2^G \mathbf{N}_m u_m - w) \\ -(v\mathbf{Y} - \mathbf{N}_O - 2^G \mathbf{N}_m u_m)\end{aligned} \tag{6}$$

where $\mathbf{Y}$ is a vector of p components all equal to 1. The dependency of $\mathbf{A}$ on the unknown quantities u_M, u_m, w, and v is linear; hence, the system of four equations is linear, which satisfies the criterion of the linear least-squares problem. Rearranging the vector $\mathbf{A}$ of (6) as

$$\mathbf{A} = u_M(\mathbf{n}\mathbf{N}_M) + u_m\left[\mathbf{N}_m - (\mathbf{n}\mathbf{N}_m)\right] - w\mathbf{n} - v\mathbf{Y} + \mathbf{N}_O \tag{7}$$

and noting the vector

$$\mathbf{M} = \begin{pmatrix} (\mathbf{n}\mathbf{N}_M) \\ \mathbf{N}_m - (\mathbf{n}\mathbf{N}_m) \\ \mathbf{n} \\ \mathbf{Y} \end{pmatrix} \tag{8}$$

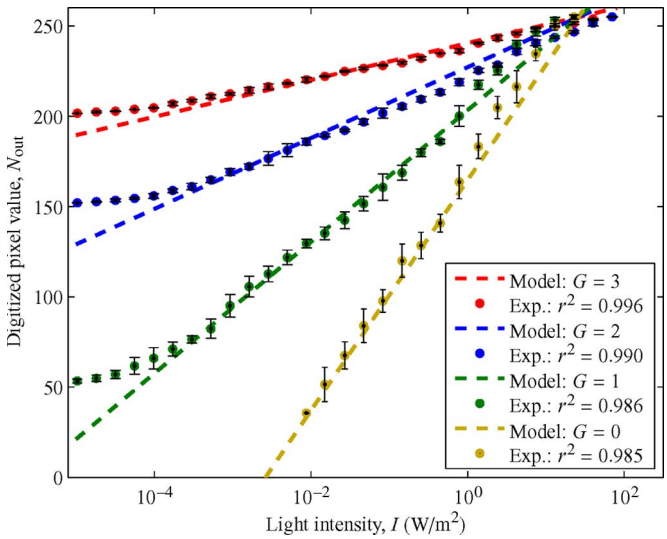

Fig. 5. Digitized camera output and input light intensity: a comparison of the model with experimental data.

the vector $\mathbf{A}$ can be rewritten using (4) and (8) in the form of a matrix as

$$\mathbf{A} = \mathbf{XM} + \mathbf{N}_O \tag{9}$$

and the quantity to be minimized becomes

$$\mathbf{A}^2 = \mathbf{A} \cdot \mathbf{A} = (\mathbf{MX} + \mathbf{N}_O)(\mathbf{MX} + \mathbf{N}_O)^{\mathrm{T}} = 0$$
$$\Rightarrow \mathbf{M}^{\mathrm{T}}(\mathbf{MX} + \mathbf{N}_O) = 0 \tag{10}$$

where $\cdot$ represents the matrix dot product, and W^{T} represents the transpose of a matrix W. From (10), the unknown quantities of (4) are solved through

$$\mathbf{X} = [\mathbf{MM}^{\mathrm{T}}]^{-1}\left[\mathbf{M}^{\mathrm{T}}(-\mathbf{N}_O)\right]. \tag{11}$$

In Fig. 5, the model that relates the 8-bit digitized camera output to the input light intensity is compared with the experimental data. With rms error values less than 2 pixel grayscale levels at each value of gain over an 8-bit output, the model is accurate within 0.8%. In an experimental situation, the camera parameter gain G, offset N_O, and digitizer settings $\mathrm{ADC}_{\max}$ and $\mathrm{ADC}_{\min}$ are known. Using the parameter extraction technique described above, it is possible to relate the 8-bit pixel value to the analog voltage of the CMOS sensor and hence to the value of light intensity on the pixel. The importance of this is related to (2), where the pixel speed of response and hence the maximum camera frame rate are determined by the input light intensity.

III. CMOS-DSP Camera in WLI

WLI [11] uses a low temporal coherence light source that has the property that interference is only achieved when the sample and reference paths are matched within the coherence length of the source. Therefore, by translating one arm of the interferometer, the depth information of the sample is attained, and a 3-D image of the sample can be noninvasively constructed. In a Michelson interferometer employing a white-light source, the intensity produced by the recombination of light from the reference and sample arms can be written as

$$I_{\mathrm{WLI}} = I_{\mathrm{dc}} + I_{\mathrm{ac}} \tag{12}$$

where I_{dc} and I_{ac} will be expressed terms of the source intensity I_L and the reference and sample reflectivity constants k_1 and k_2, where $k_1 = {B_1}^2 R_R$, and $k_2 = {B_2}^2 R_S$. Here, R_R and R_S are the sample and reference light power reflectivities, respectively, and B_1 and B_2 are the beam power splitting ratios with $B_1 + B_2 \approx 1$. The dc and ac light intensity components of the WLI signal from (12) are defined as

$$I_{\mathrm{dc}} = k_1 I_L + k_2 I_L \tag{13}$$

$$I_{\mathrm{ac}} = 2\sqrt{(k_1 I_L)(k_2 I_L)}\,|\gamma_{\mathrm{SR}}(\Delta t)| \cos\left|\left[\alpha_{\mathrm{SR}} - \delta_{\mathrm{SR}}(\Delta t)\right]\right. \tag{14}$$

where $\gamma_{\mathrm{SR}}(\Delta t)$ is the complex degree of coherence of the two waves, and $|\gamma_{\mathrm{SR}}(\Delta t)|$ is their degree of coherence. The term $\delta_{\mathrm{SR}}(\Delta t) = 2\pi\bar{\nu}\Delta t$ is the phase delay, $\Delta t = \Delta z/c$ is the time delay, Δz is the path difference between the beams, $\bar{\nu}$ is the mean spectral frequency of the light source, and c is the speed of light. The term α_{SR} is a constant phase. Here, I_{WLI} is called the "WLI signal," and $|\gamma_{\mathrm{SR}}(\Delta t)|$ is called the "WLI envelope." The WLI envelope has a Gaussian shape determined by the bandwidth of the light source and is written as

$$|\gamma_{\mathrm{SR}}(\Delta t)| = \exp\left[-\left(\frac{\pi\Delta\nu\Delta t}{2\sqrt{\ln 2}}\right)^2\right] \tag{15}$$

where $\Delta\nu$ is the optical frequency bandwidth. The WLI envelope is the signal of interest in profile measurements utilizing WLI, since its magnitude represents the reflectivity of a specific point in or on the sample, and its peak is the precise axial location.

By translating one arm of the interferometer, both the axial scanning can be achieved and an electronically detectable Doppler-shifted optical carrier is generated. The speed of the translation determines the speed of the scanning and hence the frequency of the Doppler-shifted carrier, which is defined as

$$f_D = \frac{2\bar{\nu}v_s}{c} \tag{16}$$

where v_s is the scanning speed or path length variation. Therefore, the WLI signal of (12) is on a sinusoidal carrier dependent upon the scanning speed of the interferometer. Fig. 6 shows a simulated WLI envelope with its Doppler-shifted carrier. When detecting a WLI signal with a logarithmic CMOS-DSP camera, the dc component of the signal must be considered since the pixel speed of response is dependent upon the light intensity.

A. Digitized Output Signal Amplitude

To analyze the output magnitude of the WLI envelope when detected by the camera, the output voltage of the CMOS

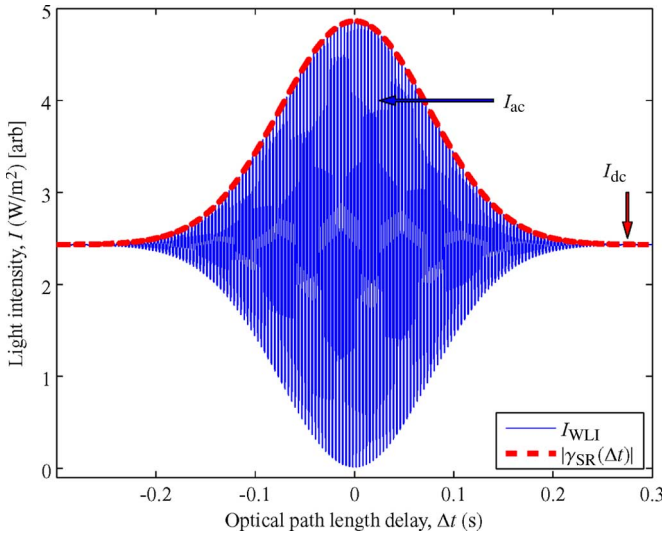

Fig. 6. Simulated WLI signal with $\bar{\lambda} = 830$ nm, $\Delta\lambda = 14$ nm, and $f_D = 300$ Hz.

sensor to the WLI signal is obtained by incorporating (12) into (1), thus

$$V_{\mathrm{WLI}} = m\log_{10} \times\left\{\frac{I_L}{I_0}(k_1+k_2)+\frac{I_L}{I_0}2\sqrt{(k_1k_2)}|\gamma_{\mathrm{SR}}(\Delta t)|\cos(2\pi f_D\Delta t)\right\} \tag{17}$$

where the Doppler-shifted carrier has replaced the optical frequency $\bar{\nu}$, and the constant phase α_{SR} has been omitted from (14). The output voltage of the CMOS sensor of (17) can be rewritten as

$$V_{\mathrm{WLI}} = m\log_{10}\left\{\frac{I_L}{I_0}\right\} + m\log_{10} \times\left\{(k_1+k_2)+2\sqrt{(k_1k_2)}|\gamma_{\mathrm{SR}}(\Delta t)|\cos(2\pi f_D\Delta t)\right\}. \tag{18}$$

It is evident that due to the logarithmic response of the sensor, the WLI envelope term $|\gamma_{\mathrm{SR}}(\Delta t)|$ is independent of the source intensity I_L. Moreover, since the output of the camera is a process of digitizing (18) with equal level spacing through (3), the magnitude of the WLI envelope is determined by the ratio of the ac to dc component of the light intensity, i.e., the interference fringe visibility

$$\begin{aligned} F &= \frac{\sqrt{(k_1I_L)(k_2I_L)}}{(k_1I_L)+(k_2I_L)} \\ &= \frac{\sqrt{k_1k_2}}{\sqrt{I_L}(k_1+k_2)} \\ &= \frac{\sqrt{(R_RB_1^2)\,(R_SB_2^2)}}{\sqrt{I_L}\,[(R_RB_1^2)+(R_SB_2^2)]}. \end{aligned} \tag{19}$$

Hence, increasing the source intensity will in fact decrease the amplitude of the coherence envelope at the digitized camera output. In the WLI of a rough surface having low light power reflectivity ($R_S \approx 0.1\%$), this quantity is maximized when $k_1 = k_2$, i.e., $R_R = B_2 = 1 - R_S$.

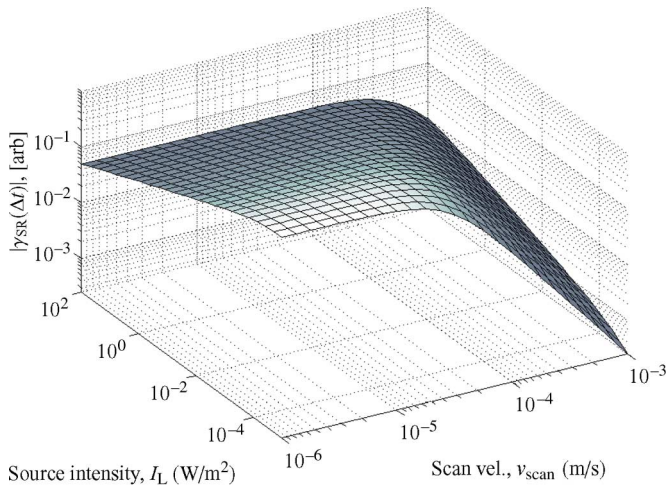

Fig. 7. Inherent tradeoff between the WLI envelope magnitude, scanning speed, and source intensity when using the camera in WLI.

Therefore, in utilizing the camera in WLI, a fundamental tradeoff exists between the WLI envelope magnitude, the scanning speed, and the source intensity. The scanning speed is limited by (2), where low intensities force a low scanning speed. Increasing the source intensity does not increase the magnitude of the WLI envelope, as demonstrated in (18), but as a property of the logarithmic response, the WLI envelope magnitude decreases from (19). This relationship is shown in Fig. 7 for a mathematical simulation using the 830-nm superluminescent diode (SLD) with the experimentally verified frequency response model of (2) and the pixel output model of (3). The scanning velocity v_s assumes a 200-μm scan depth. It is evident that increasing either the source intensity or the scanning speed of the interferometer results in the output WLI envelope decreasing.

B. Sensitivity of a Logarithmic CMOS-DSP Camera in Optical Coherence Tomography

The temporal noise in the camera was experimentally verified as being independent of light intensity over a 22-dB range, as shown in Fig. 8. Using maximum amplification, i.e., $G = 0$, the average noise level in terms of pixel grayscale levels was 1.16 rms or a 0.95-dB noise level over the 120-dB range of the camera. The application of the camera to optical coherence tomography is limited by its logarithmic response and high noise level. To obtain the WLI envelope, the peak-to-peak digitized pixel amplitude of the envelope must be greater than the digitized pixel rms noise. This can be expressed, using the ac and dc intensity components of the WLI signal of (12), as

$$I_{\mathrm{ac}} > (100 + 10^{N_{\mathrm{rms}}})I_{\mathrm{dc}}. \tag{20}$$

In the case of the camera investigated in this paper with $N_{\mathrm{rms}} = 1.16$, the peak-to-peak intensity of the WLI signal must be greater than 16% of the dc light intensity. In optical coherence tomography, where there is a relatively strong reflection from

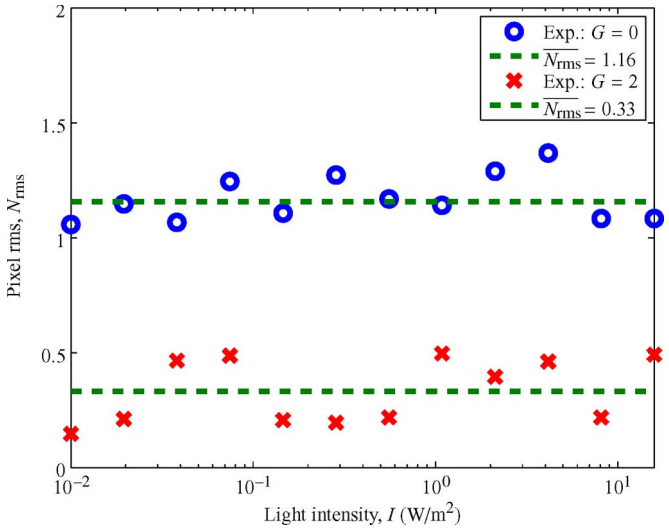

Fig. 8. Temporal noise in the CMOS pixel is relatively independent of the light intensity.

the sample surface, any subsample microstructure that reflects less than 16% of this value cannot be imaged.

IV. Conclusion

A comprehensive modeling of a logarithmic CMOS-DSP camera and its application to full-field WLI has been presented. The logarithmic voltage response, pixel response time, and relationship between CMOS sensor output voltage and camera 8-bit digital output have been mathematically modeled and verified through simulation and experimental data. The logarithmic response, high noise level, and slow pixel response time at low intensities limit its application to the full-field profilometry of rough surfaces, since in optical coherence tomography the subsample microstructure with a reflectivity of less than 16% of the surface reflectivity cannot be resolved. However, its direct readout, region-of-interest imaging, and fast frame rates are advantageous in optical metrology and machine vision applications, where light power is ample, and an inexpensive, autonomous, and versatile imaging device is demanded.

References

[1] P. Egan, F. Lakestani, M. P. Whelan, and M. J. Connelly, "Full-field optical coherence tomography with a complimentary metal–oxide semiconductor digital signal processor camera," *Opt. Eng.*, vol. 45, no. 1, pp. 015 601.1–015 601.6, Jan. 2006.

[2] J. M. Schmitt, "Optical coherence tomography (OCT): A review," *IEEE J. Sel. Topics Quantum Electron.*, vol. 5, no. 4, pp. 1205–1215, Jul./Aug. 1999.

[3] S. Kavadias, B. Dierickx, D. Scheffer, A. Alaerts, D. Uwaerts, and J. Bogaerts, "A logarithmic response CMOS image sensor with on-chip calibration," *IEEE J. Solid-State Circuits*, vol. 35, no. 8, pp. 1146–1152, Aug. 2000.

[4] S. Fischer, N. Schibli, and F. Moscheni, "Design and development of the smart machine vision sensor (SMVS)," in *Proc. SPIE—Advanced Focal Plane Arrays Electronic Cameras II*, Zurich, Switzerland, Sep. 1998, vol. 3410, pp. 186–192.

[5] J. Little, "Random access CMOS imaging technology applied to an industrial machine vision problem," in *Proc. IEE Semin. On-line Monitoring Tech. Off-Shore Ind.*, May 1999, vol. 143, pp. 9/1–9/2.

[6] H. Helmers and M. Schellenberg, "CMOS vs. CCD sensors in speckle interferometry," *Opt. Laser Technol.*, vol. 35, no. 8, pp. 587–595, Nov. 2003.

[7] M. V. Aguanno, F. Lakestani, M. P. Whelan, and M. J. Connelly, "Heterodyne speckle interferometer for full-field velocity profile measurements of a vibrating membrane by electronic scanning," *Opt. Lasers Eng.*, vol. 45, no. 6, pp. 677–683, Jun. 2007.

[8] D. Joseph and S. Collins, "Modeling, calibration, and correction of nonlinear illumination-dependent fixed pattern noise in logarithmic CMOS image sensors," *IEEE Trans. Instrum. Meas.*, vol. 51, no. 5, pp. 996–1001, Oct. 2002.

[9] T. Lulé, S. Benthien, H. Keller, F. Mütze, P. Rieve, K. Seibel, M. Sommer, and M. Böhm, "Sensitivity of CMOS based imagers and scaling perspectives," *IEEE Trans. Electron Devices*, vol. 47, no. 11, pp. 2110–2122, Nov. 2000.

[10] W. H. Press, S. A. Teukolsky, W. T. Vetterling, and B. P. Flannery, *Numerical Recipes in C: The Art of Scientific Computing*, 2nd ed. New York: Cambridge Univ. Press, 2002.

[11] M. Born and E. Wolf, *Principles of Optics: Electromagnetic Theory of Propagation, Interference and Diffraction of Light*, 7th ed. Cambridge, U.K.: Cambridge Univ. Press, 1999.

Patrick Egan received the B.Eng. and Ph.D. degrees from the University of Limerick, Limerick, Ireland, in 2003 and 2006, respectively. His doctoral research studies were carried out in collaboration with the European Commission Joint Research Centre, Italy, and were chiefly concerned with optical profilometry and its application to machine vision and mechanical testing.

He is currently with the Optical Communications Research Group, Department of Electronic and Computer Engineering, University of Limerick. His research interests include several topics in the field of optical instrumentation, measurement, and metrology.

Fereydoun Lakestani received the degree in engineering from Ecole Nationale Supérieure d'Electronique et de Radioélectricité de Grenoble, Grenoble, France, in 1971 and the Doctorate degree in science from the Institut National des Sciences Appliquées de Lyon, Lyon, France.

For 13 years, he was with the Institut National des Sciences Appliquées de Lyon, where he taught physics and nondestructive techniques. Since 1984, he has been with the European Commission Joint Research Centre, Ispra, Italy. His research activities until 1997 were in various fields of ultrasonic applications, e.g., transducers, NDT, material characterization, and medicine. From 1997 to 2001, he worked on thermal waves. Since 2001, he has been involved in various applications of laser interferometry. Throughout his research activities, he has acquired skill in ultrasonic, optical, and thermal wave propagation, and the use of electronic instrumentation, signal processing, and data analysis.

Maurice P. Whelan received the Doctorate degree in computational and experimental stress analysis from the University of Limerick, Limerick, Ireland, in 1994.

He is currently the Head of the Photonics Sector with the European Commission Joint Research Centre, Ispra, Italy, and an Adjunct Professor with the Stokes Research Institute, University of Limerick. He is the author of 13 international patents. He has worked on the development and application of full-field optical metrology techniques, optical fiber sensing, and biomedical imaging. His current interests include interference microscopy for cell and tissue diagnostics *in vitro*, hyperspectral fluorescence imaging for endoscopy, and optical waveguide biosensors.

Michael J. Connelly (S'89–M'92) received the Ph.D. degree in electronic engineering from the University College Dublin, Dublin, Ireland, in 1991.

He is currently a Senior Lecturer in electronic engineering with the University of Limerick, Limerick, Ireland, where he leads a research group working on optoelectronic device modeling, all-optical signal processing using semiconductor optical amplifiers, optical coherence tomography, and optical metrology.